Molecular Dynamics Simulation of Surfactin Derivatives at the Decane/Water Interface at Low Surface Coverage

Hong-Ze Gang, Jin-Feng Liu, and Bo-Zhong Mu*

State Key Laboratory of Bioreactor Engineering and Institute of Applied Chemistry, East China University of Science and Technology, Shanghai, China 200237

Received: September 24, 2009; Revised Manuscript Received: December 27, 2009

Interfacial behavior of surfactin methyl ester derivatives at the *n*-decane/water interface at low surface coverage has been studied by molecular dynamics simulation. Molecular orientations, structural variability of the peptide ring backbones, interfacial molecular areas, and the motion activities of surfactin derivatives have been determined. The simulations show that surfactin monomethyl ester stands vertically at the oil/water interface compared with surfactin molecule. The aliphatic chains tilt at the interface and can fold back to interact with the hydrophobic amino acid residues within the same molecule. Amino acid residues that the aliphatic chains are favorable to interact with are different between surfactin derivatives. The peptide ring backbones of surfactin and surfactin derivatives expand at the interface. Interfacial molecular areas of surfactin derivatives are all about 110 Å^2. Translational and rotational motions of surfactin derivatives are limited at the interface, and the motion activities increase with the hydrophobic character of the peptide moiety.

1. Introduction

Surfactin, a family of cyclic lipopeptides produced by several strains of *Bacillus subtilis*, is considered as one of the most powerful biosurfactants. Surfactin exhibits a prominent surface activity since it reduces the surface tension of aqueous solution from 72 to 27 mN m^{-1} at a concentration of 20 μM.[1] Extensive studies demonstrated that surfactin also showed biological activity, such as antibacterial,[2] antiviral,[2,3] antifungal,[4] hemolytic,[3] and membrane activities.[5,6] Surfactin consists of a heptapeptide with a typical amino acid sequence of L-Glu-L-Leu-D-Leu-L-Val-L-Asp-D-Leu-L-Leu bonded to a β-hydroxy fatty acid and closed via a lactone bond. Carbon atom in the β-hydroxy fatty acid moiety was reported in a number range of 12−17.[7−9] 3-D conformation of the peptide ring was characterized to adopt a "horse-saddle" topology in DMSO solution.[10] The two acidic amino acid residues were close to each other and formed a hydrophilic domain on one side of the molecule, and the hydrophobic domain on the opposite side was populated by the aliphatic chain and most of the hydrophobic amino acid residues.

Surfactin methyl ester derivatives can be naturally produced[11] and chemically synthesized,[12] and it was reported that the methyl esterification of the carboxyl in acidic amino acid residue had significant effect on the antiviral, hemolytic, and surface activities of surfactin.[3,12,13] Early studies showed that the antiviral and hemolytic activities of surfactin monomethyl ester were more efficient than that of surfactin.[2,3,12] Experimental studies of Thimon and co-workers[12] showed that the surface activity of surfactin-Glu-γ-methyl ester was higher than that of surfactin, as the γ_{cmc} reached 31 mN m^{-1} instead of 34 mN m^{-1} for surfactin. The cmc was considerably decreased, namely 30 μM instead of 240 μM for surfactin. The cmc value of surfactin dimethyl ester could not be determined since the compound almost completely lost its water solubility, but the oil displacement results showed that the surface activity of surfactin dimethyl ester elevated by 20% higher than that of surfactin.[13] Moreover, surfactin dimethyl ester could retain similar activities irrespective of pH change, though surfactin activity drastically decreased from alkaline conditions to acidic conditions. The promotion of surface activity of surfactin methyl ester was attributed to the reduction of carboxyl group in peptide moiety and a consequent decrease of the repulsive charge between molecules, and therefore the micellization was enhanced and a more compact aggregate was easily formed on the surface.[12] Nevertheless, the understanding of methyl esterification of carboxyl in hydrophilic amino acid residue and its effect on surfactin surface activity is still limited.

Surface activity mainly occurs at interfaces and is governed by the conformational state of molecules at hydrophobic/hydrophilic interface. In this paper, a *n*-decane/water medium was employed to mimic a hydrophobic/hydrophilic biphasic system, and the interfacial behaviors of surfactin methyl esters were studied using molecular dynamics simulation. Molecular orientations, structural variabilities of the peptide ring backbones, the motion activities and the interfacial molecular areas were evaluated, and the data resulting from surfactin methyl esters were compared with that of surfactin for better understanding the role of methyl esterification of the carboxyl in their surface activity.

2. Model Setup and Simulation Method

Molecules in this simulation were all described by explicit all-atom model and the MMFF94 force field[14−18] was employed to calculate both the internal and external interactions. The total potential energy has the form

* To whom correspondence should be addressed. Tel: +86-21-64252063. Fax: +86-21-64252458. E-mail: bzmu@ecust.edu.cn. Postal address: East China University of Science and Technology, Mailbox 424, 130 Meilong Road, Shanghai, China 200237.

10.1021/jp909202u
Published on Web 02/05/2010

$$E_{tot} = \sum E_B + \sum E_A + \sum E_{BA} + \sum E_{OOP} + \sum E_T + \sum E_{vdW} + \sum E_Q \quad (1)$$

where E_{tot}, E_B, E_A, E_{BA}, E_{OOP}, E_T, E_{vdW}, and E_Q are the total potential energy and the bond stretching, angle bending, stretch−bend interactions, out-of-plane bending at tricoordinate centers, torsion interaction, van der Waals, and electrostatic components, respectively. Energy functions' details are given as follows:

$$E_B = 143.9325\frac{K_B}{2}\Delta r^2\left(1 + cs\Delta r + \frac{7}{12}cs^2\Delta r^2\right) \quad (2)$$

$$E_A = 0.043844\frac{K_A}{2}\Delta\theta^2(1 + cb\Delta\theta) \quad (3)$$

$$E_{BA} = 2.51210(K_{BA1}\Delta r_1 + K_{BA2}\Delta r_2)\Delta\theta \quad (4)$$

$$E_{OOP} = 0.043844\frac{K_{OOP}}{2}\chi^2 \quad (5)$$

$$E_T = 0.5[K_{T1}(1 + \cos\phi) + K_{T2}(1 - \cos(2\phi)) + K_{T3}(1 + \cos(3\phi))] \quad (6)$$

$$E_{vdW} = \varepsilon\left(\frac{1.07R_{ij}}{r_{ij} + 0.07R_{ij}}\right)^7\left(\frac{1.12R_{ij}^7}{r_{ij}^7 + 0.12R_{ij}^7} - 2\right) \quad (7)$$

$$E_Q = 332.0716\frac{q_iq_j}{Dr_{ij}} \quad (8)$$

where K_B, K_A, K_{OOP}, K_{BA}, and K_T are the bond stretching, angle bending, out-of-plane bending, bond stretch coupled angle bending, and torsion interaction force constants, respectively; Δr and $\Delta\theta$ are the difference between actual bond length and reference bond length and the difference between actual bond angle and reference bond angle, respectively; χ and ϕ are the out-of-plane angle and dihedral angle, respectively. A buffered 14−7 form was employed to describe the van der Waals interaction between atoms i and j belonging to separate molecules or separated by three or more chemical bonds. R_{ij}, ε, q_i, D and r_{ij} are the minimum energy separation, the well depth, partial charge of atom i, dielectric constants, and the distance between atom i and j, respectively. In each case, units of energy, distance, and angle are in kcal mol^{-1}, angstroms, and degrees, respectively. Electrostatic interactions were computed using Ewald sum.[19]

Figure 1 shows the primary structures of surfactin and surfactin derivatives. Here, surfactin is *iso*-C15 surfactin (ST-I15), and 15 denotes the number of carbon atoms in the fatty acid moiety. Surfactin derivatives are all derived from *iso*-C15 surfactin; they are surfactin dimethyl ester (ST-1M5M), surfactin-Glu-γ-methyl ester (ST-1M5E), surfactin-Asp-β-methyl ester (ST-1E5M), and surfactin sodium salt (ST-1E5E).

The peptide ring backbones of surfactin and surfactin derivatives adopt a "horse-saddle" conformation proposed by Bonmatin,[10] and the two acidic amino acid residues orientate on the opposite direction of hydrophobic aliphatic chain which is in an extended conformation. Take ST-I15 for example; its

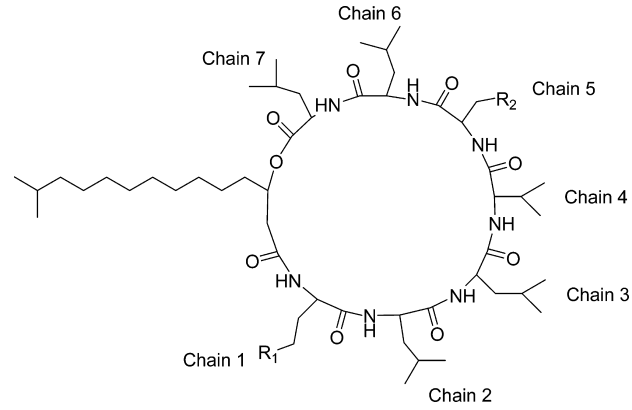

	ST-I15	ST-1M5M	ST-1M5E	ST-1E5M	ST-1E5E
R_1	COOH	$COOCH_3$	$COOCH_3$	COO^-Na^+	COO^-Na^+
R_2	COOH	$COOCH_3$	COO^-Na^+	$COOCH_3$	COO^-Na^+

Figure 1. Primary structures of surfactin and surfactin derivatives.

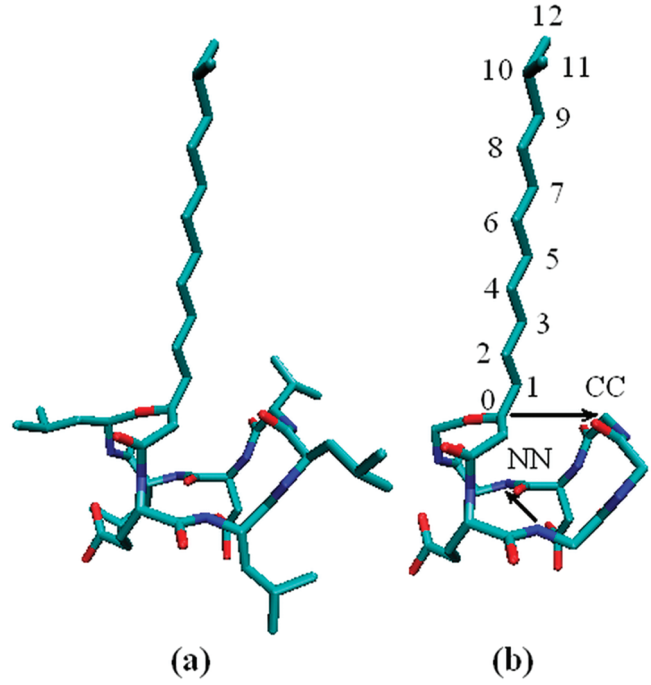

Figure 2. (a) Secondary structure of ST-I15; for visual clarity, the hydrogen atoms are not displayed. (b) Definition of **CC** and **NN** vectors in the ST-I15 head group and the carbon-atom-assigned sequence in hydrophobic aliphatic chain, for visual clarity, the hydrophobic residues on the peptide ring are not displayed. The atom coloring scheme is C, green; N, blue; and O, red. Conformation graphs in this paper are all produced with VMD software.[20] Conformations of the heptapeptide ring backbones, vector definitions, and atom-assigned sequences of surfactin derivatives are the same as that of ST-I15 molecule.

secondary structure is shown in Figure 2a. The aliphatic chain that away from the peptide ring (from carbon atom 1) is taken as surfactant tail and the residual moiety is taken as surfactant head group.

All the systems have the same setup steps. First, we equilibrated a box containing water molecules with its L_x and L_y size was 38 Å × 38 Å, and then set the box to the center of a cell which had the same L_x and L_y dimensions as the initial box. Second, 14 surfactant molecules were applied on the water surface with a concentration of 7 molecules per surface. The surfactant molecules were positioned on the water surface with their peptide rings laid flat at the surface, the two acidic amino

acid residues inserted into water and the hydrophobic tail protruded to the vacuum, and a short run of 10 ps with small step was performed to eliminate the exclusion between water molecules and surfactant molecules as well as to randomize the conformations of the hydrophobic aliphatic chains. Finally, with the cell filled with *n*-decane molecules, a small time step was applied at the beginning of the equilibrium process and then was gradually increased to a value of 1 fs. The simulation process was continued at least 250 ps to achieve equilibrium. The equations of motion were solved by Verlet velocity algorithm, and Berendsen thermostat[21] was used to control the temperature. All the systems had the same composition: 245 decane molecules, 14 surfactant molecules, and 1928 water molecules, nearly total 16 000 atoms. The cell dimension in the z direction was about ~112 Å, and the periodic boundary condition was applied to all three spatial directions. The cutoff radius of both van der Waals interactions and the real part of electrostatic interactions was 9 Å. After the equilibrium had been achieved, the MD trajectories were stored every 0.1 ps during a 1.0 ns run. All the simulations were performed at constant temperature (293.15 K) and volume (NVT ensemble).

3. Results

3.1. Density Profiles and Interface Location. The simulation cells were divided into slabs along z coordinate, and the atomic density profiles of water, *n*-decane and surfactant were calculated according with

$$\rho\langle z\rangle = \frac{\langle m_i \delta(z - z_i)\rangle}{V_{\text{slab}}} \tag{9}$$

Take the *n*-decane/ST-I15/water system as example, the density profiles are shown in Figure 3a. We observe from the figure that both ST-I15 and surfactin derivatives (not shown) molecules reside at the *n*-decane/water interface. Significant separation between the hydrophobic tail and the head group indicates that the surfactant tails protrude into the oil phase due to the hydrophobic interactions between *n*-decane molecules and hydrophobic aliphatic tails.

Density profiles of water and *n*-decane can be respectively fitted into a hyperbolic tangent functional form[22]

$$\rho(z) = \frac{1}{2}(\rho_{\text{L}} + \rho_{\text{V}}) \pm \frac{1}{2}(\rho_{\text{L}} - \rho_{\text{V}}) \tanh[(z - z_0)/d] \tag{10}$$

where ρ_{L} and ρ_{V} are the liquid and vapor densities, respectively, z_0 denotes the position of the interface, and d is a measure of the width of the interface. As shown in Figure 3b, 10−90 criteria are applied to identify the interface region of the aqueous phase as well as that of the oil phase, and the *n*-decane/water interface region is located between position of 90% of bulk decane density and position of 90% of bulk water density.

3.2. Surfactant Orientations. In order to investigate the orientations of hydrophilic head groups and hydrophobic aliphatic chains of surfactin and surfactin derivatives at the *n*-decane/water interface, we first define several vectors in surfactant molecules. As shown in Figure 2b, carbon atoms in hydrophobic aliphatic chains are assigned in the sequence of 0, 1, ..., 10, 11, and 12 from the β carbon atom. The vector that connects C0 and C10 was defined as the end-to-end **Tail** vector of the aliphatic chain, and the vectors connecting C0 and Cn are defined as **Tn** vectors. The **CC** vector is defined as the vector

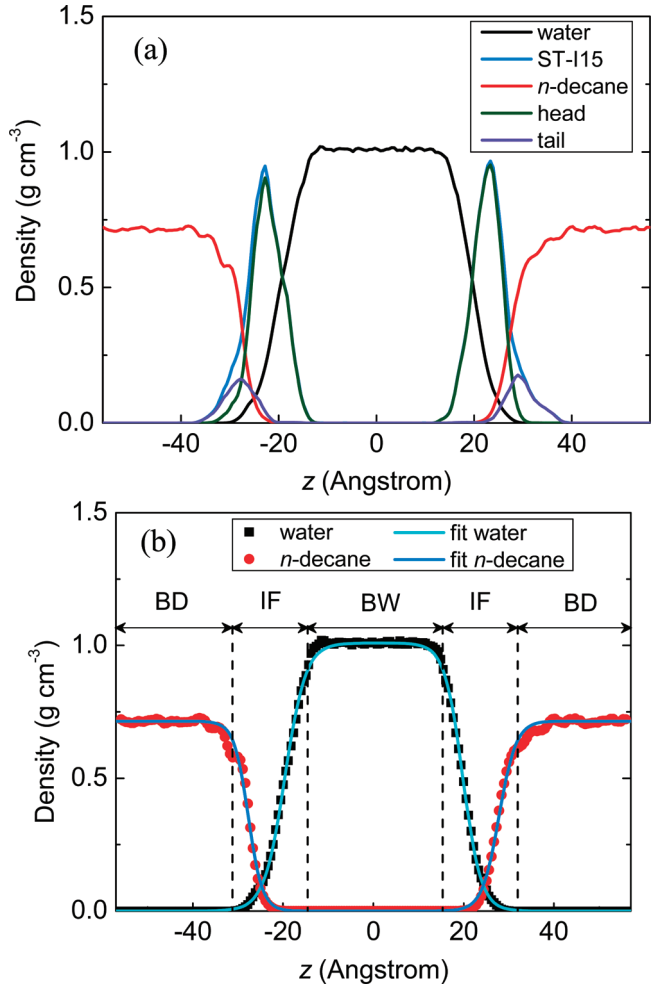

Figure 3. (a) Density profiles and (b) interface region location of *n*-decane/ST-I15/water system, where BD, IF, and BW denote bulk decane, interface region, and bulk water, respectively.

connecting the β carbon atom of the fatty acid (C0) and the α carbon atom in chain 4 (CH(4)), the vector that connects the nitrogen atom of chain 2 (NH(2)) and the nitrogen atom of chain 6 (NH(6)) is defined as the **NN** vector. Carbon atoms of C0 and CH(4) correspond to the two top points of the hydrophobic side of the horse-saddle conformation, while nitrogen atoms of NH(2) and NH(6) represent the two top points of the hydrophilic side of the horse-saddle conformation of the peptide ring.

The orientations of surfactant molecules were studied by measuring the angle between the vectors in surfactant molecules, $\vec{R}$, and the normal to the plane of *n*-decane/water interface, $\vec{n}$ (from bulk water to bulk decane).The orientational cosine is in the form of

$$\cos\alpha = \frac{\vec{R} \cdot \vec{n}}{|\vec{R}|} \tag{11}$$

The angular distributions were calculated by taking an average over all the surfactant molecules at the *n*-decane/water interface. Figure 4a shows the normalized probability distributions of α_{CC}. It is clear that the distribution of each α_{CC} is broad. The main contribution of angular distribution of ST-I15 is in the range of 75−150°, and the main contributions >90° of α_{CC} are observed for surfactin derivatives except ST-1E5M. The angular distribution of α_{CC} indicates that the **CC** vectors of surfactin and surfactin derivatives tilt at the oil/water interface, **CC** vectors

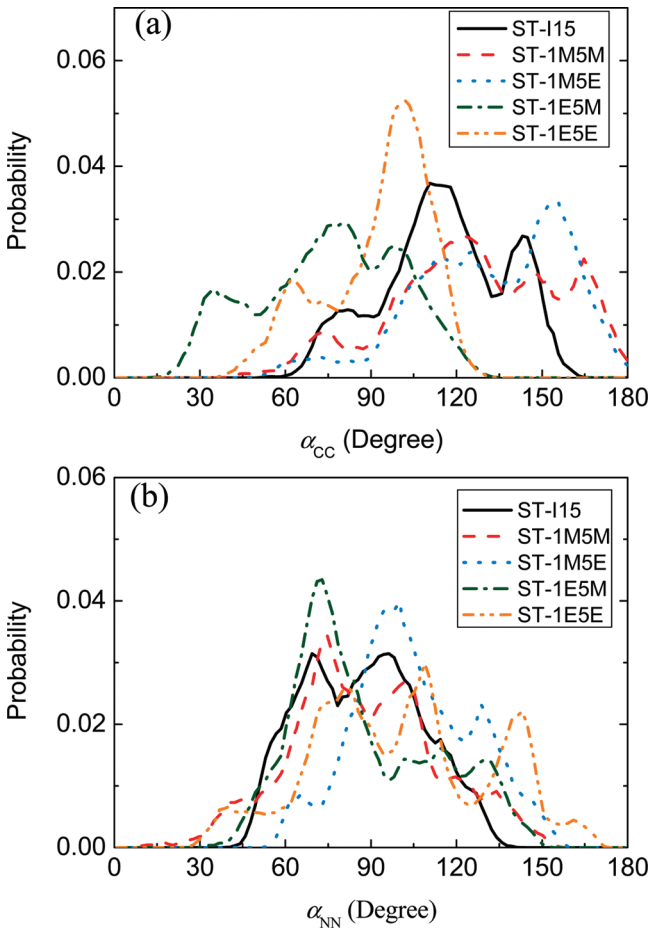

Figure 4. Normalized probability distribution of (a) α_{CC}, the angle of the **CC** vectors in surfactant head groups with respect to the normal to the interface, and (b) α_{NN}, the angle of the **NN** vectors in surfactant head groups with respect to the normal to the interface, $\vec{n}$.

except those of ST-1E5M point to aqueous phase. A main peak centered on 90−115° of ST-1E5E suggests that the orientations of **CC** vectors nearly parallel the interface. As shown in Figure 4b, broad distributions of α_{NN} for ST-I15 and ST-1M5M are centered on the value of 90°. For ST-1M5E, the main angular distribution driftes toward high angle value comparing with that of ST-I15, while the main angular distribution of ST-1E5M drifts toward low angle value. The drifts of the angular distribution of ST-1M5E and ST-1E5M demonstrate that the **NN** vectors tilt at the interface.

From the orientations of both **CC** vectors and **NN** vectors in head groups of surfactant molecules, we can conclude that the surfactin monomethyl esters stand vertically at the interface, especially the peptide rings of ST-1M5E, while the peptide rings of ST-1E5E nearly lie flat at the interface. Snapshots of the representative orientations of the peptide rings of surfactin and surfactin derivatives are displayed in Figure 5.

The orientations of the hydrophobic aliphatic chains of surfactants can be explained by the probability distribution of α_{Tail}, the angle of the end-to-end **Tail** vectors with respect to the normal to the interface, $\vec{n}$. As shown in Figure 6, the angular distributions of α_{Tail} are in a range of 0−90° for surfactin and surfactin derivatives, and the main peaks center on 0−30°. Contributions <45° to the angular distribution of ST-1E5E are higher than that of surfactin and surfactin methyl ester.

To obtain further insight of the individual probability distribution of each vector in the aliphatic chains, the average values of the angle, α_{Tn}, between **Tn** vectors and the normal to the interface were calculated and shown in Figure 7. It is clear that the average value of α_{Tn} first decreases (for $n < 5$) and then increases gradually with the number sequence of carbon atoms in aliphatic chains of ST-I15, ST-1E5M, and ST-1E5E. The rising tendency of the average value of α_{Tn} after $n > 5$ indicates a larger deviation of the aliphatic chains from the normal to the oil/water interface. The average value of α_{Tn} of ST-1M5E molecules nearly keeps constant with the increase of the carbon atom number, suggesting a similar inclination of each **Tn** vector. The rising tendency of the average value of α_{Tn} of ST-1M5M indicates that the terminal part of the aliphatic chain is rather close to the oil/water interface.

As can be seen in Figure 6, the hydrophobic aliphatic chains of surfactants swing within a large scale and could come close to the oil/water interface in some cases, and these orientations make it possible for the hydrophobic contact between the aliphatic chains and the hydrophobic side chains within the same molecule. Instances where the aliphatic chains folded back to interact with the hydrophobic amino acid residues had been found in these simulations. A criterion specific to the hydrophobic contact between surfactants molecules[23] was employed to identify these hydrophobic interactions between aliphatic tails and side chains. Surfactant conformations were screened to select the conformations that a hydrophobic atom in the aliphatic chains was located within 3.5 Å from a hydrophobic atom in the side chains within the same molecule, and the hydrophobic atom here was defined as all carbon atoms except those in carboxylate (COO^-) groups. The percents of conformations represented the hydrophobic contact between the aliphatic chains and side chains are plotted in Figure 8. It is clear that the hydrophobic characters of chain 1 and chain 5 greatly influence the priority of the hydrophobic contact between the aliphatic chain and each side chain.

During the process of folding back to the peptide ring, nearly half of the aliphatic chains of ST-I15 interact with chain 7 (L-Leu), the others intend to interact with chain 3 (D-Leu) and chain 4 (L-Val), which are on the other top point of the hydrophobic side of the horse-saddle conformation. For ST-1E5M and ST-1E5E with negative charge in chain 1, hydrophobic contact between aliphatic chains, and chain 7 decrease, chain 3 and chain 4 are the side chains that the aliphatic chains are favorable to interact with, while in ST-1M5M and ST-1M5E, besides chain 3 and chain 4, hydrophobic contacts mostly appear between the aliphatic chains and chain 1. In particular, the larger inclination of the peptide ring of ST-1M5E at the interface leads to the aliphatic chains associating more easily with chain 1 than with other side chains. Hydrophobic contact between aliphatic chain and chains 2 and 6 is scarcely detected, and this can be ascribed to the opposite positions of chain 2 and chain 6 compared with that of the aliphatic chains. Conformations of surfactin and surfactin derivatives that represent the hydrophobic contacts between the aliphatic chains and the side chains within the same molecule are displayed in Figure S1 of the Supporting Information.

3.3. Structural Variability of the Peptide Ring Backbone.

The average lengths of the **CC** and **NN** vectors are measured to estimate the spans of the hydrophobic and the hydrophilic side of the horse-saddle conformation and the results are given in Table 1. It shows in the table that **CC** vectors and **NN** vectors of surfactin and surfactin derivatives at the decane/water interface appear in a length increase of nearly 30%, suggesting more expanded and flat structures of the peptide rings compared with the original structure.

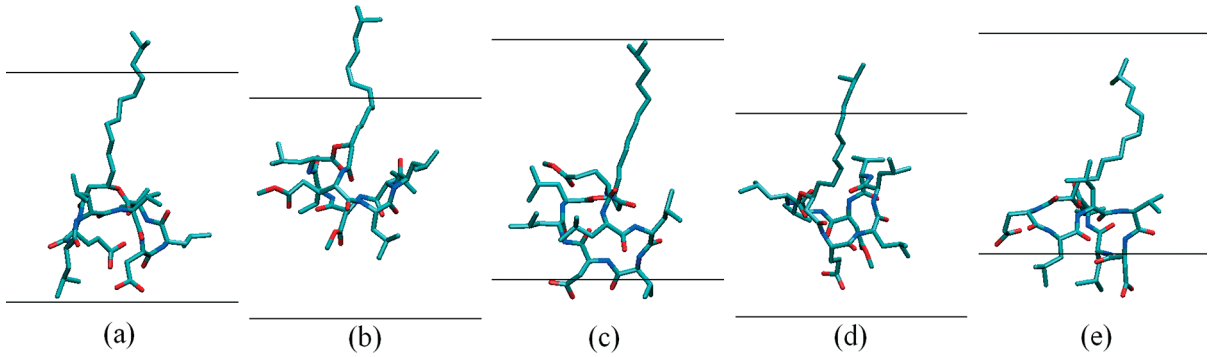

Figure 5. Snapshots of representative orientations of the peptide ring of (a) ST-I15, (b) ST-1M5M, (c) ST-1M5E, (d) ST-1E5M, and (e) ST-1E5E at the *n*-decane/water interface. The black lines denote the boundaries of interface region in each system. For visual clarity, the hydrogen atoms and sodium ions are not displayed.

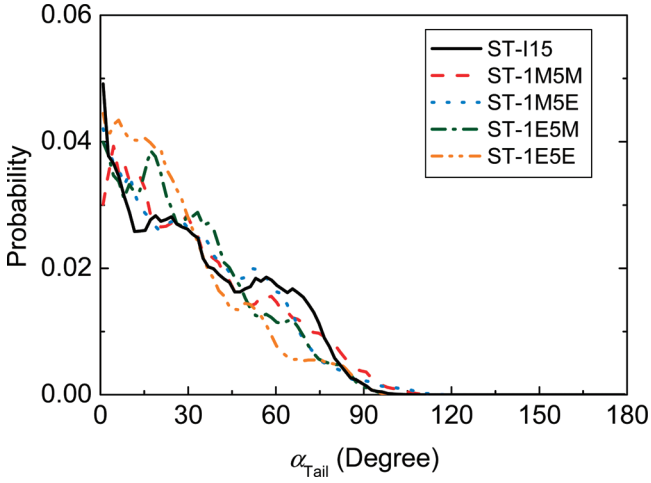

Figure 6. Normalized probability distribution of α_{Tail}, the angle of the end-to-end **Tail** vectors in hydrophobic aliphatic chains with respect to the normal to the interface, $\vec{n}$.

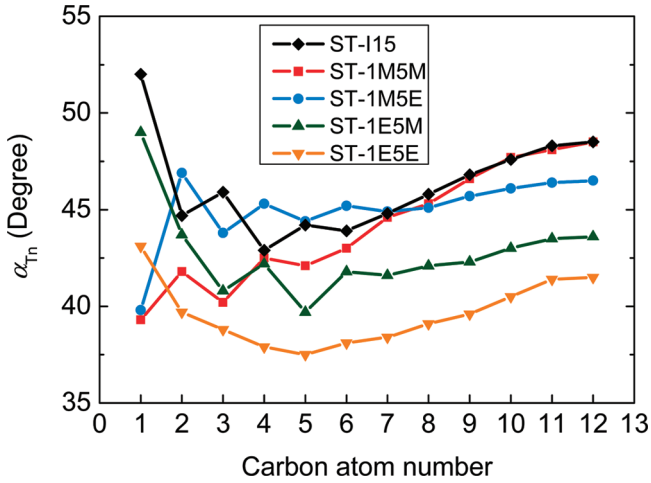

Figure 7. Average value of the angle, α_{Tn}, between **Tn** vector in hydrophobic aliphatic chains of surfactant molecules and the normal to the interface, $\vec{n}$.

In order to investigate the structural variability of the peptide rings at the interface, especially the effect of chemical modification of the two acidic amino acid residues on the horse-saddle conformation, root mean square deviations of the peptide ring backbones from its original structure ($rmsd_0$) and from the average structure ($rmsd_1$) were estimated. The data (rmsd values of surfactin and surfactin derivatives are listed in Table S1 of the Supporting Information) demonstrate that the rmsd of the peptide rings in the same system are different between molecules. $Rmsd_0$ of the peptide rings of surfactin and surfactin derivatives are generally in a range of 0.7−2 Å compared with their original structure. It can be concluded that the peptide ring backbone has a tiny conformational change when $rmsd_0$ is within 1.1 Å; as can be seen in Figure 9a, the peptide ring backbone of one ST-I15 molecule, that with a $rmsd_0$ of 0.754 Å, nearly holds its original conformation. As displayed in Figure 9b, peptide ring backbone with a higher $rmsd_0$ value adopts a more expanded horse-saddle structure, while the $rmsd_1$ of surfactin and surfactin derivatives are within a value of 0.6 Å and fluctuate within a narrow range, suggesting that the structures of the backbones are stable at the oil/water interface.

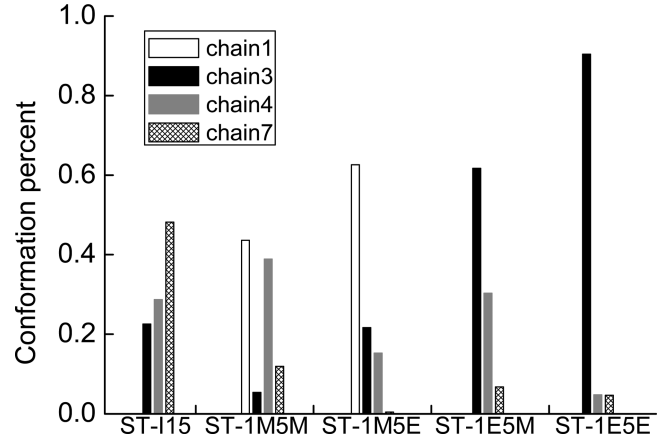

Figure 8. Conformations represented the hydrophobic contact between the hydrophobic aliphatic chain and the side chains within the same molecule.

TABLE 1: Average Lengths (in Å) of CC Vectors and NN Vectors[a]

surfactant	|CC|	|NN|
original	4.6	5.5
ST-1M5M	6.0 ± 1.5	7.5 ± 1.5
ST-1M5E	5.9 ± 1.4	7.3 ± 1.6
ST-1E5M	6.1 ± 1.6	7.2 ± 1.6
ST-1E5E	7.0 ± 1.8	7.0 ± 1.2
ST-I15	6.2 ± 1.3	7.2 ± 1.3

[a] The standard deviations were calculated by averaging over both time origins and the surfactant molecules.

3.4. Surfactant Assembles. Intermolecular structure of surfactin and surfactin derivatives at the oil/water interface were estimated by calculating the two-dimensional radial distribution functions (tRDFs)[24] of the center of mass of surfactant head groups. The tRDFs is defined as

$$g(r) = \frac{\sum_{i,j} \delta(r - r_{ij})}{2\pi r \, \mathrm{d}r \, \rho^{\mathrm{IF}}}; \quad r_{ij} = \sqrt{x_{ij}^2 + y_{ij}^2} \qquad (12)$$

where ρ^{IF} is the average number density of surfactant molecule at the interface plane. It is clearly shown in Figure 10 that the maximum of the first peak of tRDFs of ST-1E5E is at 14.5 Å, and the first peaks of other surfactants are observed at 12−13 Å. A larger separation between head groups of ST-1E5E is caused by the electrostatic repulsion between the negative charges in different molecules, and the minimum of the intermolecular distance, lower than 9 Å, can be obtained between ST-1M5E molecules largely due to the larger inclination of the peptide ring at the interface, which induces a close-packing arrangement of surfactant molecules.

3.5. Interfacial Molecular Area. By measuring the projection of surfactant molecules onto the oil/water interface, interfacial areas A1−A5 are obtained, which are the average interfacial areas of the heptapeptide ring (including all atoms on the peptide ring backbone and atoms bonded to the backbone), the side chains (including all atoms in head group excluding the atoms in A1), the whole head group, the hydrophobic aliphatic chain, and the whole surfactant molecule, respectively.

As given in Table 2, the interfacial areas of the peptide rings of surfactin and surfactin derivatives, A1, are in a range of 50−60 Å^2. The lowest value of A1 is obtained for ST-1M5E,

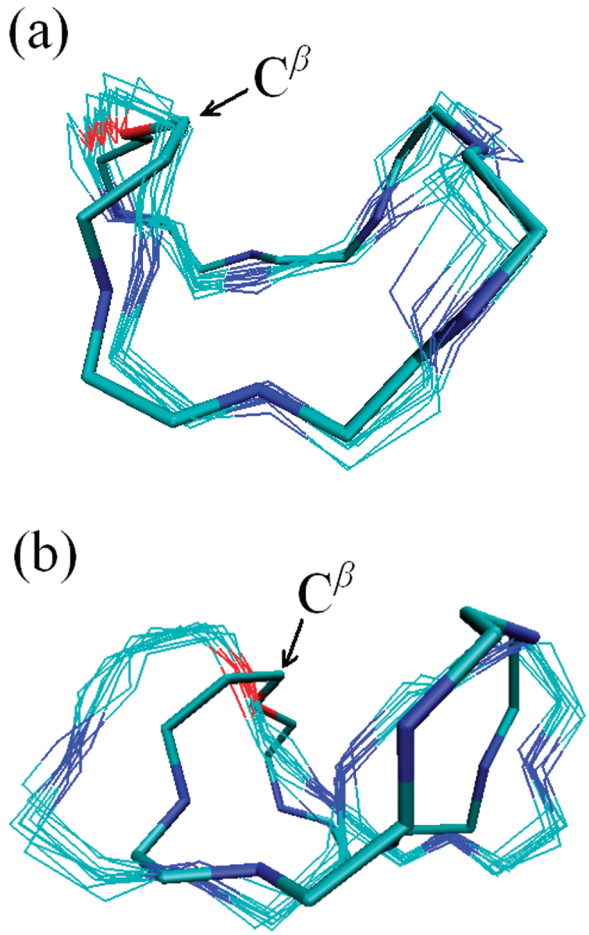

Figure 9. Alignment of the peptide ring backbone of ST-I15 between original structure (stick) and 10 structures (line) captured during the product period every 0.1 ns, where the rmsd$_0$ is (a) 0.754 ± 0.073 Å and (b) 1.690 ± 0.181 Å.

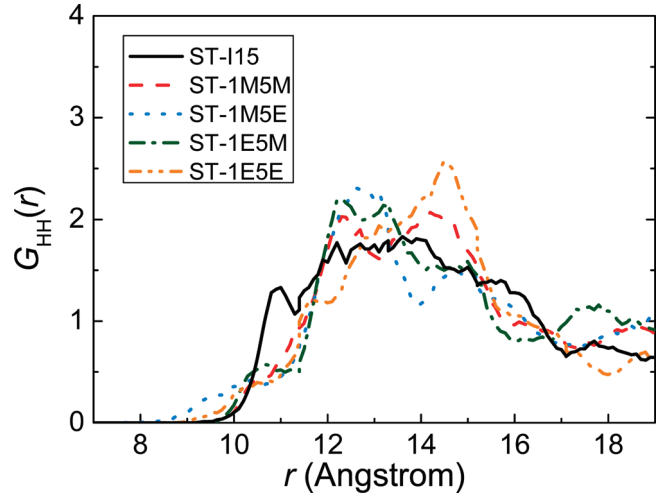

Figure 10. Two-dimensional radial distribution functions, $G_{\mathrm{HH}}(r)$, of the center of mass of the surfactant's head groups.

the peptide ring of which has the largest inclination at the interface. The order of A3 value is greatly different from the order of the A1 value, indicating that the orientations and the compositions of the side chains strongly affect the interfacial areas of the head groups. A4 values of surfactin and surfactin derivatives are similar for the same composition, and it can be easily judged that the aliphatic chains of ST-1E5E that have the lowest value of A4 are more tilted than other surfactants, and this result confirms the previous discussion of Figure 6. The interfacial molecular areas of surfactin and surfactin derivatives at the oil/water interface, A5, mainly depend on the interfacial area of head group and are all about 110 Å^2.

3.6. Dynamical Properties of Surfactin and Surfactin Derivatives. The mean square displacements (MSDs) of the mass centers of head groups and hydrophobic aliphatic chains according to the Einstein relation were calculated to estimate the translational activity of surfactant. Since the amphiphilic molecules inhabit the *n*-decane/water interface, we separately calculated the MSDs both in the tangential direction and in the normal direction of the *xy* plane.[25,26] The tangential and normal diffusion coefficients, D_{T} and D_{N}, deduced from the slope of the linear fit line of MSDs are listed in Table 3. The normal translational coefficients of surfactant head groups are much lower than the tangential translational coefficients, demonstrating a strong anisotropy of the translational motion of surfactant molecules at the interface. Translational motions of head groups in the normal direction of the *xy* plane are limited by the strong polar interactions between head groups and water molecules. Comparing with surfactant head groups, the translational diffusion coefficients of the aliphatic chains are a little higher for their small volume and simple structure.

The rotational activities of surfactant molecules were studied by detecting the reorientational dynamics of their head groups. Because of the complex structure of the head groups, rotational dynamics of many vectors in the head group were monitored to obtain an accurate result.[27] Eight vectors are defined in the head group and their reorientational time correlation functions are calculated as follows:[28]

$$C_{\mathrm{R}}(t) = \frac{\langle \hat{b}(t+\tau) \cdot \hat{b}(\tau) \rangle}{\langle \hat{b}(\tau) \cdot \hat{b}(\tau) \rangle} \qquad (13)$$

where $\hat{b}$ is the defined vector in surfactant head group, and the final reorientational dynamics of the head group is obtained by

TABLE 2: Interfacial Areas (in Å^2) of Surfactin and Surfactin Derivatives at the Oil/Water Interface[a]

surfactant	A1	A2	A3	A4	A5
ST-1M5M	56.0 ± 9.2	57.6 ± 2.5	98.9 ± 8.8	23.1 ± 3.4	112.4 ± 9.5
ST-1M5E	53.8 ± 7.7	56.5 ± 2.4	97.6 ± 7.1	22.9 ± 3.4	111.5 ± 7.6
ST-1E5M	60.1 ± 8.2	55.1 ± 3.0	96.9 ± 8.7	22.6 ± 3.5	111.2 ± 8.3
ST-1E5E	60.2 ± 8.1	52.8 ± 2.3	95.1 ± 8.4	22.1 ± 3.5	110.2 ± 9.8
ST-I15	55.9 ± 9.1	54.6 ± 2.8	94.7 ± 9.8	23.1 ± 3.5	108.3 ± 12.0

[a] The standard deviations were calculated by averaging over both time origins and the surfactant molecules.

TABLE 3: Translational Diffusion Coefficients (in 10^{-6} cm^2 s^{-1}) of the Head Groups and Hydrophobic Aliphatic Chains of Surfactin and Surfactin Derivatives[a]

	head group		tail	
surfactant	D_T	D_N	D_T	D_N
ST-1M5M	3.782 ± 0.308	1.135 ± 0.262	3.014 ± 0.560	0.644 ± 0.090
ST-1M5E	3.298 ± 0.513	0.622 ± 0.095	4.512 ± 0.230	1.208 ± 0.011
ST-1E5M	3.075 ± 1.414	0.492 ± 0.117	4.600 ± 1.287	1.110 ± 0.021
ST-1E5E	2.334 ± 0.019	0.502 ± 0.110	3.306 ± 0.189	1.032 ± 0.244
ST-I15	2.818 ± 0.513	0.508 ± 0.053	4.340 ± 0.573	1.318 ± 0.018

[a] The error estimates were calculated from the average values of two 0.5 ns long trajectories.

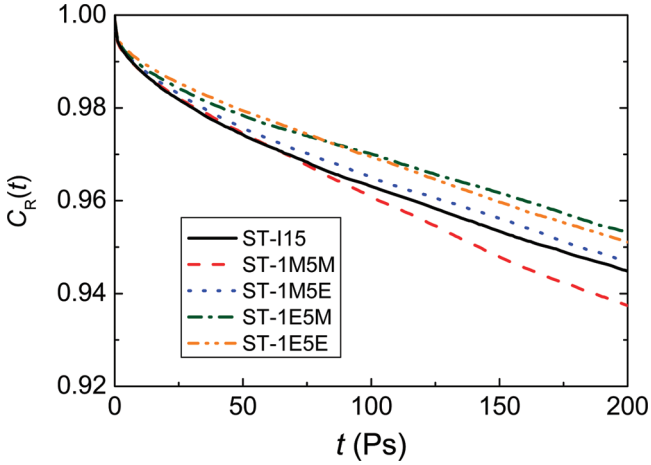

Figure 11. Reorientational dynamics of the head groups of surfactin and surfactin derivatives.

averaging the reorientational time correlation functions of these eight vectors. It is clearly shown in Figure 11 that the reorientational motion of surfactant head groups at the interface is so slow for the strong polar interactions between water molecules and the hydrophilic groups in the peptide moiety. The relaxation time of reorientational motion of surfactant decreases with the increase of the hydrophobic character of the head group. The relaxation of ST-1M5M is the fastest, while the reorientational times of ST-1E5E and ST-1E5M are a little longer.

3.7. Structural and Dynamical Properties of Interfacial Water. The structure of water molecules around surfactant head groups can be described by radial distribution functions (RDFs) of oxygen atoms on the peptide ring backbone (Oc), nitrogen atoms on the peptide ring backbone (N), and oxygen atoms on side chains (Os) with oxygen atoms in water molecules (Ow). RDFs of Oc, N, and Os with Ow normalized by bulk water density are shown in Figure 12a−c. Well-defined peaks are obtained for all RDFs, suggesting that the head groups of surfactin and surfactin derivatives intensively influence the structure of water molecules around them. The maximum of the first peak in $G_{OcOw}(r)$ and $G_{NOw}(r)$ are at 2.67 and 2.82 Å, respectively. It can be predicted that the peptide ring backbones of ST-1E5E and ST-1M5E go more deeply into the aqueous phase according to the values of RDFs in Figure 12a,b at large coordinate of r. As shown in Figure 12c, the neighboring water of Os in ST-1E5E molecules is the highest, and chain 1 and chain 5 go deeply into bulk water. In contrast, the neighboring water of Os in ST-1M5M molecules is the lowest and both chain 1 and chain 5 are more far away from bulk water for their higher hydrophobic character.

To distinguish the translational activities of water molecules in interface region from that in bulk region, we determined the translational diffusion coefficient of interfacial water as well as bulk water. The Einstein relation for interfacial water can be written in the form of[29]

$$D_T = \lim_{t\to\infty} \frac{1}{4tN(t)} \langle [x(t+\tau) - x(\tau)]^2 + [y(t+\tau) - y(\tau)]^2 \rangle \quad (14)$$

$$D_N = \lim_{t\to\infty} \frac{1}{2tN(t)} \langle [z(t+\tau) - z(\tau)]^2 \rangle \quad (15)$$

where the ensemble average is over all water molecules that reside in the interface region during the time between 0 and $t + \tau$. $N(t)$ is the number of data points that contribute to the average at time t, and $N(t)$ takes into account the fact that when a water molecule crosses the boundaries between interface region and bulk region, its time variables t and τ are set to zero.

As given in Table 4, the translational diffusion coefficients of interfacial water are extremely lower than that of bulk water, since the translational motion of interfacial water is significantly slowed down by the strong polar interactions between surfactants and water molecules. Anisotropy of the translational motion of water molecules in interface region is also observed, indicating the limitation of the translational motion of interfacial water in the normal direction of the interface is larger than that in the tangential direction. Tangential diffusion coefficients of interfacial water appear to increase with the hydrophobic character of the surfactant molecule, while the normal diffusion coefficients, D_N, are suggested to relate to the orientation of the head group of surfactants at the interface.

4. Discussion

The hydrophobic interactions between decane molecules and the surfactant aliphatic chains result in the rise of the peptide

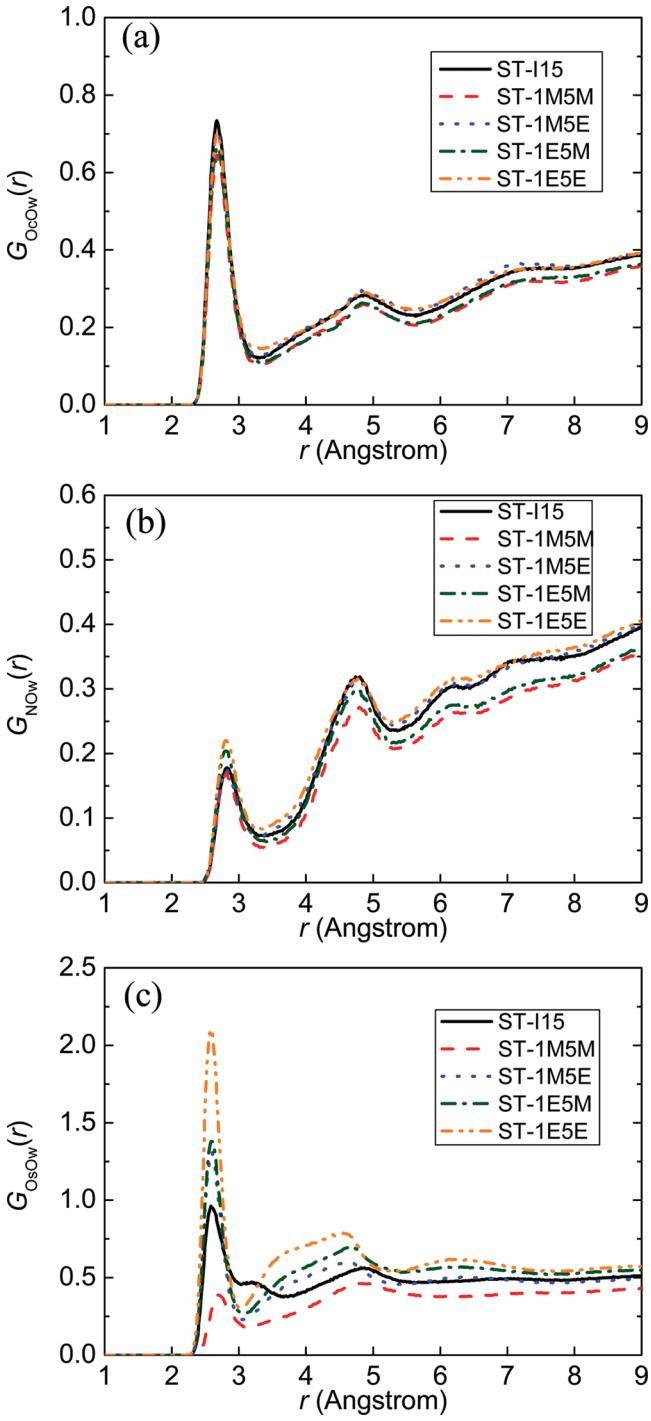

Figure 12. Radial distribution functions of the (a) oxygen atoms (Oc) on the peptide ring backbone, (b) nitrogen atoms (N) on the peptide ring backbone, and (c) oxygen atoms (Os) in chain 1 and chain 5 with water oxygen atoms Ow, normalized by the bulk water density.

ring segment that contain C0 from the oil/water interface, and gain a > 90° main contribution of α_{CC} distribution for ST-I15 molecules. The orientations of **CC** vectors of ST-I15 agree reasonably well with previous studies of Nicolas.[30] It was shown that the α_{CC} distribution of surfactin molecules at the *n*-hexane/water interface was in the range of 60−150°. It can be easily identified from the definitions of **CC** vector and **NN** vector in Figure 2b that chain 1 resides between the initial point of **CC** vector and the initial point of **NN** vector, and chain 5 resides between the terminal point of **CC** vector and the terminal point of **NN** vector, and therefore, the different hydrophobic character

TABLE 4: Translational Diffusion Coefficients (in 10^{-5} cm^2 s^{-1}) of Water Molecule[a]

	interfacial water		bulk water
surfactant	D_T	D_N	D
ST-1M5M	1.119 ± 0.003	0.475 ± 0.002	2.585 ± 0.062
ST-1M5E	1.031 ± 0.135	0.404 ± 0.028	2.519 ± 0.102
ST-1E5M	0.973 ± 0.174	0.434 ± 0.010	2.503 ± 0.017
ST-1E5E	0.888 ± 0.020	0.485 ± 0.066	2.426 ± 0.018
ST-I15	1.107 ± 0.043	0.517 ± 0.002	2.500 ± 0.019

[a] The error estimates were calculated from the average values of two 0.5 ns long trajectories.

between chain 1 and chain 5 leads to the tilted orientations of **CC** and **NN** vectors from the interface and the consequent inclination of the peptide ring. Especially in ST-1M5E, **CC** and **NN** vectors all point to the aqueous phase as a result of the hydrophobic character of chain 1 and the hydrophilic character of chain 5; in addition, the aliphatic chain on the initial point of **CC** vector enhanced the inclination of the peptide ring at the oil/water interface.

The aliphatic chains of surfactants tilt on the oil/water interface and protrude into bulk decane as a result of the favorable interactions between the aliphatic chains and decane molecules. Similar orientation behaviors of the hydrophobic chains of surfactant at the oil/water interface were obtained both in simulation[31] and in experiment.[32] However, the orientations of surfactin aliphatic chains at the oil/water interface are quite different from those on the surface of the aqueous solution. Neutron reflectivity data[33] showed that the location of surfactin tails was nearly the same as that of residues on the peptide ring, suggesting that the surfactin aliphatic chains lay flat within the water surface.

Because of the low surface coverage of the surfactant, the hydrophobic aliphatic chains swung flexibly and sometimes interacted with the side chains within the same molecule. The phenomenon that the aliphatic chains folded over in contact with hydrophobic leucines or valine that resided on the same side of the molecule was also observed at the surface of the aqueous phase;[33] however, the amino acid residues with which the hydrophobic aliphatic chains interact were not exactly identified. Data of the conformation screening for the hydrophobic contact show that chain 3, chain 4, and chain 1 with its carboxyl methyl esterified are the side chains that aliphatic chains are favorable to interact with. The reason that aliphatic chains are more favorable to interact with chain 1 than with chain 7 in ST-1M5M and ST-1M5E can be explained by the length of chain 1 which contains the methyl ester group being larger than the length of chain 7, and chain 1 is more far away from C0, and thus the aliphatic chains can interact with chain 1 with a slighter bending of its linear structure.

Though the peptide rings of surfactin and surfactin derivatives expand at the interface, the tilted orientations of the peptide rings result in lower value of A1. The interfacial area of the surfactin peptide ring determined here is a little larger than the 50 Å^2 in studies of Bonmatin.[10,32] Interfacial molecular areas of surfactin and surfactin derivatives at the oil/water interface are lower than the 150−220 Å^2 of surfactin at the surface of aqueous solution;[34−37] this mainly due to the tilted orientations of the aliphatic chains at the interface, particularly the vertical inclination of the peptide rings of surfactin derivatives. Interfacial molecular area of surfactin at the *n*-decane/water interface at low surface coverage in this simulation is consistent with the simulation result of Gellet;[37] the interfacial molecular area of surfactin is 126−138 Å^2 at the hydrophilic/hydrophobic

interface. Although the hydrogen bonds of CO(2)−NH(5) that characterized the β-turn structure of the peptide ring were detected in surfactin and surfactin derivatives molecules, lifetimes of the hydrogen bonds were short due to the large distance between CO(2) and NH(5) caused by the structural expansion of the peptide ring backbone. Two more stable hydrogen bonds of CO(1)−NH(5) and CO(7)−NH(1) were observed in surfactin molecules and were also detected in surfactin in SDS micellar solution.[38]

The translational diffusion coefficient of ST-I15 obtained in this simulation is consistent with that at the hexane/water interface with a similar surface coverage.[30] Higher translational diffusion coefficients of ST-1M5E result from the vertical orientation of its peptide ring. Most part of the peptide ring is away from water and thus free from polar interaction with water molecules, and so ST-1M5E head groups translate more flexibly in both tangential direction and normal direction of the *xy* plane. The highest diffusion coefficients of ST-1M5M are estimated for the hydrophobic character of its head group.

Although the structural fluctuations of the peptide ring have effect on the reorientational dynamics of the head groups, the main contribution to the rotational motion is the polar interactions between head groups and water molecules. Rotational motion of ST-1E5E is accelerated by the electrostatic repulsion of the negative charges between different molecules; thus, the relaxation of ST-1E5E is a little faster than that of ST-1E5M. Most hydrophilic groups of ST-1M5E are away from the aqueous phase as a result of the vertical orientation of its peptide ring, and the limit of the rotational motion by the polar interaction reduced; thus, the reorientational time of ST-1M5E is shorter than that of ST-1E5M. The reorientational motion of ST-1M5M molecules at the oil/water interface is more flexible for the weaker interactions between the head group and water molecules.

The nearest-neighbor number of water molecules within the first hydration shell of Oc by integrating over the first peak of RDFs is larger than that of N; this can be ascribed to the difference of atom position and electron negativity between Oc and N. Nitrogen atoms are on the peptide ring while most oxygen atoms Oc bond to the carbon atoms on the peptide ring, and so N are not as exposed to water as the Oc atoms; additionally, the electron negativity of Oc is stronger than that of N, and therefore the neighboring water molecules of Oc are more than those of N, and the nearest-neighbor distance between water molecules and Oc is closer than that of N.

The hydrophobic character and the orientation of surfactant head groups are the main factors affecting the motion activity of interfacial water. The peptide ring of ST-1E5E is nearly parallel to the oil/water interface resulting in a dense distribution of the hydrophilic groups on the interface; thus, the translational motion of interfacial water in the tangential direction of the interface is efficiently limited. Similarly, a dense distribution of the hydrophilic group in normal direction of the interface is formed for the vertical orientation of the peptide rings of ST-1M5E, and the translational motion of interfacial water in tangential direction is more active. It should be noticed that bulk water here includes those nearby the interface region, and therefore the statistic diffusion coefficients of bulk water are more or less influenced by the anisotropy of interface region; as a result, the translational diffusion coefficients of bulk water are a little lower than those determined by experiment.

The vertical orientations of surfactin monomethyl ester at the hydrophobic/hydrophilic interface benefiting the insertion of molecules into membrane are supposed to account for their excellent biological activities, since the penetration of surfactin molecule in the membrane has been proposed to be the first step of the membrane solubilization.[39]

5. Conclusions

These simulations are the first atomistic MD studies of surfactin methyl ester derivatives in a liquid hydrophobic/hydrophilic medium. The data resulting from surfactin derivatives were compared with that of surfactin for better understanding of the methyl esterification of the carboxyl effect on the structural and dynamical properties of surfactin. The simulations indicated that the peptide rings of surfactin monomethyl ester stood vertically at the oil/water interface, and the peptide ring of surfactin-Glu-γ-methyl ester had the highest inclination from the interface. Hydrophobic aliphatic chains of surfactin derivatives tilted at the interface, and in some cases folded back to interact with the hydrophobic side chains within the same molecule. Chain 3 (D-Leu), chain 4 (L-Val), and chain 1 with its carboxyl methyl esterified were the side chains that hydrophobic aliphatic chains were favorable to interact with. Different deformation of the peptide ring backbone of surfactin derivatives at the oil/water interface was detected, exhibiting more expanded and flat horse-saddle structures of the backbone. At a low surface coverage, interfacial molecular areas of surfactin derivatives at the oil/water interface were all of 110 Å^2. The translational and rotational motion of surfactant molecules at the interface were largely slowed down by the strong polar interactions between surfactants and water molecules, and the motion activities increased with the methyl-esterified groups in the peptide moiety.

The simulations present direct information of the structural and dynamical properties of surfactin methyl ester at the oil/water interface, and the results will be helpful for better understanding of the surface activities of surfactin methyl ester derivatives.

Acknowledgment. This work has been supported by the National Natural Science Foundation of China (Grant No. 50744016) and the Department of Science and Technology Shanghai (Grant No. 071607014).

Supporting Information Available: Snapshots of hydrophobic contacts between aliphatic chains and hydrophobic side chains within the same molecule, and root mean square deviations of the peptide ring backbones. This material is available free of charge via the Internet at http://pubs.acs.org.

References and Notes

(1) Peypoux, F.; Bonmatin, J. M.; Wallach, J. *Appl. Microbiol. Biotechnol.* **1999**, *51*, 553.
(2) Vollenbroich, D.; Ozel, M.; Vater, J.; Kamp, R. M.; Pauli, G. *Biologicals* **1997**, *25*, 289.
(3) Kracht, M.; Rokos, H.; Ozel, M.; Kowall, M.; Pauli, G.; Vater, J. *J. Antibiot.* **1999**, *52*, 613.
(4) Tendulkar, S. R.; Saikumari, Y. K.; Patel, V.; Raghotama, S.; Munshi, T. K.; Balaram, P.; Chattoo, B. B. *J. Appl. Microbiol.* **2007**, *103*, 2331.
(5) Carrillo, C.; Teruel, J. A.; Aranda, F. J.; Ortiz, A. *Biochim. Biophys. Acta* **2003**, *1611*, 91.
(6) Heerklotz, H.; Seelig, J. *Biophys. J.* **2001**, *81*, 1547.
(7) Liu, X. Y.; Yang, S. Z.; Mu, B. Z. *J. Pept. Sci.* **2008**, *14*, 864.
(8) Li, Y. M.; Haddad, N. I.; Yang, S. Z.; Mu, B. Z. *Int. J. Pept. Res. Ther.* **2008**, *14*, 229.
(9) Hue, N.; Serani, L.; Laprevote, O. *Rapid. Commun. Mass. Spectrom.* **2001**, *15*, 203.
(10) Bonmatin, J. M.; Genest, M.; Labbe, H.; Ptak, M. *Biopolymers* **1994**, *34*, 975.

(11) Liu, X. Y.; Yang, S. Z.; Mu, B. Z. *Process Biochem.* **2009**, *44*, 1144.
(12) Thimon, L.; Peypoux, F.; Das, B. C.; Wallach, J.; Michel, G. *Biotechnol. Appl. Biochem.* **1994**, *20*, 415.
(13) Morikawa, M.; Hirata, Y.; Imanaka, T. *Biochim. Biophys. Acta* **2000**, *1488*, 211.
(14) Halgren, T. A. *J. Comput. Chem.* **1996**, *17*, 490.
(15) Halgren, T. A. *J. Comput. Chem.* **1996**, *17*, 520.
(16) Halgren, T. A. *J. Comput. Chem.* **1996**, *17*, 553.
(17) Halgren, T. A.; Nachbar, R. B. *J. Comput. Chem.* **1996**, *17*, 587.
(18) Halgren, T. A. *J. Comput. Chem.* **1996**, *17*, 616.
(19) Smith, W. *Comput. Phys. Commun.* **1992**, *67*, 392.
(20) Humphrey, W.; Dalke, A.; Schulten, K. *J. Mol. Graphics* **1996**, *14*, 33.
(21) Berendsen, H. J. C.; Postma, J. P. M.; Vangunsteren, W. F.; Dinola, A.; Haak, J. R. *J. Chem. Phys.* **1984**, *81*, 3684.
(22) Dang, L. X. *J. Chem. Phys.* **1999**, *110*, 10113.
(23) Stephenson, B. C.; Goldsipe, A.; Blankschtein, D. *J. Phys. Chem. B* **2008**, *112*, 2357.
(24) Yan, T. Y.; Li, S.; Jiang, W.; Gao, X. P.; Xiang, B.; Voth, G. A. *J. Phys. Chem. B* **2006**, *110*, 1800.
(25) Michael, D.; Benjamin, I. *J. Electroanal. Chem.* **1998**, *450*, 335.
(26) Chanda, J.; Chakraborty, S.; Bandyopadhyay, S. *J. Phys. Chem. B* **2005**, *109*, 471.
(27) Smith, P. E.; van Gunsteren, W. F. *J. Mol. Biol.* **1994**, *236*, 629.
(28) Jang, S. S.; Goddard, W. A. *J. Phys. Chem. B* **2006**, *110*, 7992.
(29) Schweighofer, K. J.; Benjamin, I. *J. Electroanal. Chem.* **1995**, *391*, 1.
(30) Nicolas, J. P. *Biophys. J.* **2003**, *85*, 1377.
(31) Chanda, J.; Bandyopadhyay, S. *J. Phys. Chem. B* **2006**, *110*, 23482.
(32) Lu, J. R.; Li, Z. X.; Thomas, R. K.; Binks, B. P.; Crichton, D.; Fletcher, P. D. I.; McmNab, J. R.; Penfold, J. *J. Phys. Chem. B* **1998**, *102*, 5785.
(33) Shen, H. H.; Thonmas, R. K.; Chen, C. Y.; Darton, R. C.; Baker, S. C.; Penfold, J. *Langmuir* **2009**, *25*, 4211.
(34) Mager-Dana, R.; Ptak, M. *J. Colloid Interface Sci.* **1992**, *153*, 285.
(35) Song, C. S.; Ye, R. Q.; Mu, B. Z. *Colloids Surf., A* **2007**, *302*, 82.
(36) Ishigami, Y.; Osman, M.; Nakahara, H.; Sano, Y.; Ishiguro, R.; Matsumoto, M. *Colloids Surf., B* **1995**, *4*, 341.
(37) Gallet, X.; Deleu, M.; Razafindralambo, H.; Jacques, P.; Thonart, P.; Paquot, M.; Brasseur, R. *Langmuir* **1999**, *15*, 2409.
(38) Tsan, P.; Volpon, L.; Besson, F.; Lancelin, J. M. *J. Am. Chem. Soc.* **2007**, *129*, 1968.
(39) Deleu, M.; Bouffioux, O.; Razafindralambo, H.; Paquot, M.; Hbid, C.; Thonart, P.; Jacques, P.; Brasseur, R. *Langmuir* **2003**, *19*, 3377.

JP909202U